ACS APPLIED MATERIALS & INTERFACES

www.acsami.org

Research Article

Eradication of Intracellular *Staphylococcus aureus* Persisters via On-Site Antibiotic Delivery by Poly(amino acid) Nanoparticles

Zibo Yin, Diandian Huang, Dongdong Zhao, Yizhen You, Jiaqi Gu, Wensheng Xie, T. Fintan Moriarty, Guofeng Li,* and Xing Wang*

Cite This: https://doi.org/10.1021/acsami.5c11777

Read Online

ACCESS | Metrics & More | Article Recommendations | Supporting Information

ABSTRACT: Intracellular *Staphylococcus aureus* persisters are a dormant bacterial subpopulation responsible for chronic and recurrent infections due to their ability to evade antibiotic treatment within host cells. However, effective strategies for eliminating these intracellular pathogens remain limited. Herein, we proposed a versatile poly(amino acid)-based platform, F(AM), for the effective eradication of intracellular *Staphylococcus aureus* persisters via on-site antibiotic delivery. The F(AM) platform exhibited dual-targeting capability toward macrophages and *Staphylococcus aureus* persisters, efficiently penetrating cellular barriers and achieving precise antibiotic delivery at intracellular bacterial niches. Sitafloxacin, rifampicin, and polymyxin B were identified from a panel of 11 antibiotic candidates and individually loaded into the F(AM) platform. The resulting nanoparticles markedly improved intracellular drug accumulation, protected antibiotics from degradation within the adverse intracellular environment, and overcame microenvironment-induced bacterial metabolic shifts. Compared with free antibiotics, the drug-loaded F(AM) nanoparticles notably improved their intracellular bactericidal activity. Collectively, this study highlights F(AM) as a robust and versatile platform for overcoming intracellular barriers and restoring antibiotic efficacy, offering a valuable tool for antipersister strategies and intracellular pharmacokinetic investigations.

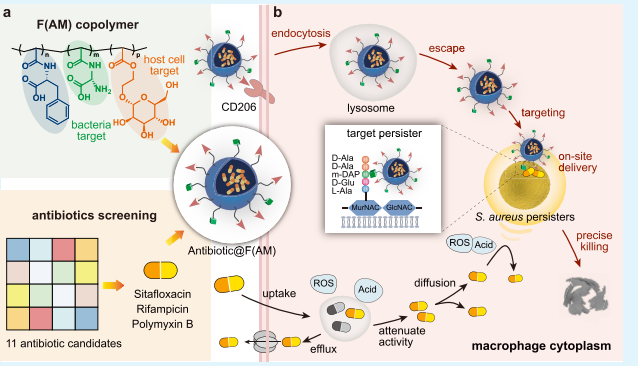

KEYWORDS: *intracellular Staphylococcus aureus, persisters, poly(amino acid) nanoparticles, on-site antibiotic delivery, intracellular pharmacokinetics of antibiotics*

1. INTRODUCTION

Intracellular bacteria manipulate host immune responses to survive, replicate, and ultimately induce host cell death.[1] They are often linked to chronic infections, including tuberculosis, meningitis, and brucellosis, which are typically resistant to high-dose and prolonged antibiotic therapy.[2−4] *Staphylococcus aureus* (*S. aureus*), classified as one of the WHO-designated "ESKAPE" pathogens, is a frequent cause of hospital- and community-acquired infections worldwide.[5−9] Although not a professional intracellular pathogen, *S. aureus* has been found to actively invade host cells to evade immune clearance and antibiotic killing, thereby establishing latent infections.[10−14] Moreover, a subpopulation of *S. aureus* enters a dormant under intracellular clearance and antibiotic exposure, which exhibit a state of nongrowth and are considered to be persisters.[15−18] Persisters represent a subpopulation of bacteria that can survive under harsh conditions.[19,20] Although they account for less than 1% of the total population, they exhibit remarkable resilience and retain the capacity to resuscitate and proliferate once antibiotic pressure is relieved,[21,22] leading to disease relapse.[23,24] Intracellular persistent *S. aureus* is recognized as a cause of recurrent infections and a major challenge for clinical care.[1,25]

Developing novel antibiotics or enhancing bactericidal effects of conventional antibiotics are main approaches to eradicate persisters.[26] For instance, chrysomycin A is a new-generation tetracycline antibiotic, which eliminates persisters by disrupting peptidoglycan synthesis and lysine precursor production;[27] The acyldepsipeptide ADEP4 activates bacterial caseinolytic peptidase P, resulting in nonspecific protease activity that targets over 400 numbers of intracellular proteins, thereby killing persistent bacteria.[28] An amphiphilic oligoamidine with a rigid structure effectively eradicates biofilm-associated persisters via a dual-targeting mechanism toward the biofilm matrix and bacterial DNA.[29] Alternatively, exogenous carbon or nitrogen sources can be administered to reactivate

Received: June 16, 2025
Revised: July 24, 2025
Accepted: August 3, 2025

Scheme 1. Construction of Antibiotic-Loaded F(AM) NPs and Their Antibacterial Performance against Intracellular *S. aureus* Persisters: (a) Construction of Antibiotic-Loaded F(AM) NPs;[a] (b) Antibiotic-Loaded F(AM) NPs Effectively Eradicate Intracellular *S. aureus* Persisters via on-Site Antibiotics Delivery[b]

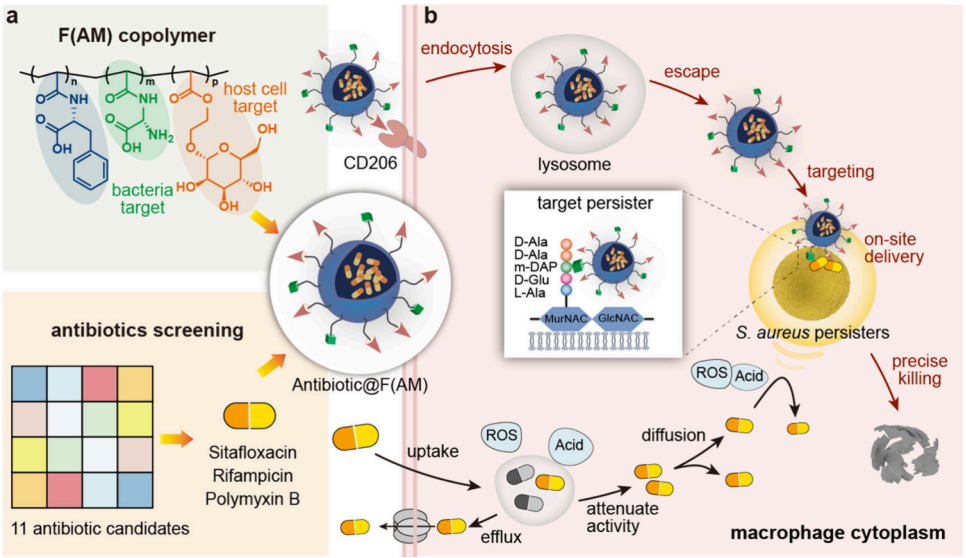

[a]Eleven antibiotics from four classes were systematically screened for their ability to eliminate intracellular persistent *S. aureus*. The screened potent antibiotics were individually encapsulated into the versatile poly(amino acid)-based platform, F(AM) to construct the final antibiotic-loaded F(AM) NPs. [b]F(AM) NPs subsequently targeted macrophage and *S. aureus* persisters mediated by mannose receptor-mediated endocytosis and peptidoglycan anchoring. Compared with the free antibiotics, F(AM) NPs markedly improved intracellular drug accumulation and protected antibiotics from degradation within the adverse intracellular microenvironment. In addition, the targeted delivery overcame microenvironment-induced bacterial metabolic shifts, ultimately restoring antibacterial activity against intracellular persisters.

metabolic activity in bacterial persisters, thereby reversing persistence and resensitizing them to conventional antibiotic killing. For instance, studies have demonstrated that supplementation with exogenous sugars enhances the tricarboxylic acid cycle in persisters, increasing proton motive force and consequently promoting intracellular uptake of aminoglycosides, which improves drug-mediated clearance of persistent populations.[30] Similarly, alkaline amino acids have been shown to resuscitate persisters and potentiate antibiotic bactericidal activity.[31,32]

However, these studies have predominantly focused on bacterial persisters in the planktonic state, with limited attention to those with intracellular niches.[33−37] Compared with planktonic persisters, the intricate intracellular microenvironment and the dynamic host-bacteria interactions impose additional constraints on the antibacterial efficacy against intracellular persisters. Host cells present multiple barriers that impede the effective intracellular activity of antibiotics. (i) Host cell membrane serves as a physical barrier that restricts antibiotic penetration into the cell and thereby reduces intracellular drug concentrations.[38−41] Moreover, efflux mechanisms actively expel antibiotics from host cells, further diminishing intracellular drug accumulation;[42,43] (ii) The intracellular microenvironment, characterized by strong acidity and high enzymatic activity, can degrade antibiotics and compromise their efficacy;[44] (iii) Complex intracellular niches, such as phagosomes, lysosomes, and the cytosol, hinders the localization and accumulation of antibiotics at bacterial sites, leading to suboptimal effective drug concentrations;[45,46] (iv) Host cells and intracellular bacteria engage in complex competitive interactions. Host cells actively restrict the availability of essential nutrients of bacteria and scavenge dead intracellular bacteria as nutrient sources;[47] In response, bacteria modulate their respiration to balance electron transport and mitigate oxidative stress imposed by host cells.[47] Thus, the intricate intracellular niche of persisters markedly differs from that of planktonic niche. Free antibiotics have limited efficacy in eliminating intracellular persistent bacteria.

Drug delivery systems represent a robust strategy for addressing intracellular bacterial infections. Our previous studies demonstrated that poly(amino acid)-based nanoparticles (NPs) facilitate the targeted delivery of antibiotics, enabling the elimination of intracellular bacteria.[48,49] However, with respect to intracellular persistent bacteria, whether targeted delivery can enhance the efficacy of drug-mediated clearance remains unresolved. Therefore, we proposed a versatile poly(amino acid)-based platform, F(AM), for the effective eradication of intracellular *S. aureus* persisters via on-site antibiotic delivery (Scheme 1). F(AM) NPs were constructed by encapsulating antibiotics within copolymers containing D-aminoalanine and mannose conjugates. These NPs employed a cascade-targeting strategy to sequentially navigate host cells and *S. aureus* persisters, delivering antibiotics directly to intracellular bacterial niches. Sitafloxacin (Sit), rifampicin (Rif), and polymyxin B (PMB) were identified from a panel of 11 antibiotic candidates across four classes. Upon delivery via the F(AM) platform, the resulting NPs markedly improved intracellular drug accumulation and protected antibiotics from degradation within the adverse intracellular microenvironment. In addition, the targeted delivery overcame microenvironment-induced bacterial metabolic shifts, ultimately restoring antibacterial activity against intracellular persisters. Specifically, Sit- and Rif-loaded F(AM) NPs elevated intracellular bactericidal rates from ∼68% (free Sit) and ∼80% (free Rif) to 96% and 92%, respectively.

https://doi.org/10.1021/acsami.5c11777
ACS Appl. Mater. Interfaces XXXX, XXX, XXX−XXX

Mechanistic studies revealed that efficacy was determined by drug accumulation, cellular stress (acidity and oxidative stress), and bacterial physiological states. Particularly, nucleic acid synthesis inhibitors like Sit exhibited inherent advantages, as persisters remained transcriptionally active but translationally repressed. Collectively, F(AM) NPs represent a robust and versatile drug delivery platform for the precise, on-site eradication of intracellular bacterial persisters. Additionally, this system offers a valuable tool for exploring intracellular antibiotic pharmacokinetics and the complex interplay between host cells and intracellular pathogens.

2. MATERIALS AND METHODS

2.1. Materials. Tryptic soy broth (TSB), luria-bertani (LB), Mueller-Hinton broth (MHB) and tryptose soy agar (TSA) were obtained from Sinopharm Chemical Reagent Co., Ltd. (China). Common solvents including dimethyl sulfoxide (DMSO), dichloromethane (DCM), ethanol (EtOH), methanol (MeOH), tetrahydrofuran (THF), trifluoroacetic acid (TFA), *m*-chlorophenyl hydrazone (CCCP), fluorescein isothiocyanate (FITC), and ethyl acetate (EA) were purchased from J&K Scientific (China). Dulbecco's Modified Eagle's Medium (DMEM) and fetal bovine serum (FBS) were purchased from Wuhan Pricella Biotechnology Co., Ltd. Other reagents used in this study, such as L-phenylalanine (≥97%), α-Boc-D-aminoalanine (≥98%), mannose (≥98%), acryloyl chloride (≥98%), α-D-mannose pentaacetate (≥97%), 2-hydroxyethyl acrylate (HEA, ≥98%), 2-(dodecylthiocarbonothioylthio)-2-methylpropionic acid (DDMAT, ≥98%), boron trifluoride diethyl etherate ($BF_3{\cdot}Et_2O$, ≥97%), tris[2-phenylpyridinato-C^2,N]iridium(III) ($Ir(ppy)_3$, ≥99%), and trimethylsilyl diazomethane ($TMSCHN_2$, ∼10% in hexane, 0.6 mol/L), were also purchased from J&K Scientific.

2.2. Synthesis of F(AM) Copolymer. The polymerization was conducted using photoinduced electron/energy transfer-reversible addition−fragmentation chain transfer (PET-RAFT) polymerization.

2.2.1. Synthesis of Monomers. The monomers α-*N*-acryloyl-phenylalanine (denoted by F), β-*N*-acryloyl-α-Boc-D-aminoalanine (denoted by A_{Boc}), and 2-(2′,3′,4′,6′-tetra-*O*-acetyl-α-D-mannosyloxy) ethyl acrylate (denoted by M_{OAc}) were synthesized according to previously reported protocols. Successful synthesis of the monomers was confirmed by ^1H nuclear magnetic resonance spectroscopy.

2.2.2. Synthesis of F(AM). Poly(α-*N*-acryloyl-phenylalanine) (denoted by PF) was first prepared via PET-RAFT polymerization. PF then served as a macro chain transfer agent (macro-CTA) for the block copolymerization of A_{Boc} and M_{OAc} to form the intermediate block copolymer poly(α-*N*-acryloyl-phenylalanine)-*block*-poly(β-*N*-acryloyl-α-Boc-D-aminoalanine-*co*-2-(2′,3′,4′,6′-tetra-*O*-acetyl-α-D-mannosyloxy) ethyl acrylate) (denoted by $F(A_{Boc}M_{OAc})$). In a typical reaction, A_{Boc} (1 g, 3.87 mmol) or M_{OAc} (1.7 g, 3.87 mmol), PF (0.83 g, 0.129 mmol), and $Ir(ppy)_3$ (25 mg, 3.87×10^{-5} mmol) were dissolved in 1 mL of DMSO. The reaction mixture was degassed with nitrogen for 30 min and then irradiated under blue light for 6 h. The resulting polymers were purified according to established procedures.

Subsequent deprotection of $F(A_{Boc}M_{OAc})$ was performed to remove both acetyl and Boc protecting groups. Specifically, $F(A_{Boc}M_{OAc})$ (220 mg) and sodium methanol (30 mg) were dissolved in 4 mL of MeOH and stirred for 4 h. The mixture was then dialyzed against methanol for 48 h using a 1000 Da dialysis membrane to yield poly(α-*N*-acryloyl-phenylalanine)-*block*-poly(β-*N*-acryloyl-α-Boc-D-aminoalanine-*co*-2-*O*-acetyl-α-D-mannosyloxy) (denoted by $F(A_{Boc}M)$). Next, $F(A_{Boc}M)$ (400 mg) was dispersed in a DCM/THF (1 mL/200 mL) mixed solution for 3 h and dialyzed in MeOH solution with 1000 Da for 48 h. The final product, F(AM), was collected and dried for further use.

Poly(α-*N*-acryloyl-phenylalanine)-*block*-poly(β-*N*-acryloyl-D-aminoalanine) (FA) was used as the control. FA was synthesized using the monomers of F and A via the same method.

2.3. Preparation of Drug-Loaded F(AM) NPs. To prepare Sit@F(AM), Rif@F(AM) and PMB@F(AM) NPs, 10 mg of F(AM) copolymer was dissolved in 1 mL of DMSO along with 1 mg of Sit, 1 mg of Rif, or 2 mg of PMB, respectively. The mixture was rapidly stirred (>1000 rpm) while 9 mL of distilled water was slowly added dropwise. After 30 min of continuous stirring, the resulting nanoparticle suspension was dialyzed against ultrapure water for 48 h. The hydrodynamic diameter, zeta potential, morphology, and colloidal stability of the NPs were subsequently characterized by dynamic light scattering (DLS) and transmission electron microscopy (TEM).

2.4. Drug Loading Capacity (DLC) And Encapsulation Rate (DLE). The DLC (%) and DLE (%) of PMB, Sit and Rif were calculated by the following equations.

$$\text{DLC (\%)} = (\text{weight of drug load}/\text{total weight of polymer and load drug}) \times 100\%$$

$$\text{DLE (\%)} = (\text{weight of drug load}/\text{total weight of drug}) \times 100\%$$

2.5. Drug Release Studies. Sit@F(AM), Rif@F(AM), PMB@F(AM) NPs were dispersed in buffer (pH 7.4 and pH 5.5) and transferred into dialysis bags (molecular weight cutoff: 3500 Da). Incubated at 37 °C with gentle shaking. At predetermined time intervals, 1 mL of the release medium was collected and replaced with an equal volume of fresh buffer. The concentrations of released Sit, Rif and PMB were determined using UV−vis spectrophotometer.

2.6. Bacterial Targeting. *2.6.1. Targeting Planktonic Bacteria or Persisters.* Exponentially growing *S. aureus* or persistent *S. aureus* were incubated with fluorescein isothiocyanate (FITC, 5 mg/mL) in saline at 37 °C for 2 h to prepare FITC-labeled bacteria (FITC-*S. aureus*). After washing three times with saline, the labeled bacteria were incubated with Nile red@F(AM) (NR@F(AM)) (10 mg/mL) for an additional 2 h. Following another three washes with saline, bacterial targeting was visualized using confocal laser scanning microscopy (CLSM).

2.6.2. Targeting Intracellular Bacteria. Exponentially growing *S. aureus* were first labeled with FITC (5 mg/mL) at 37 °C for 2 h in saline. Raw 264.7 macrophages were washed three times with PBS and then infected with FITC-*S. aureus* to construct an intracellular infection model. After infection, the macrophages were coincubated with NR@F(AM) for 6 h. For persistent intracellular bacteria, after induction of persistence, cells were similarly coincubated with NR@F(AM) (10 mg/mL) for 6 h. The macrophages were then fixed with 4% paraformaldehyde for 20 min, stained with diamidine phenyl indole (DAPI) for 5−10 min, and imaged by CLSM.

2.7. Planktonic Antibacterial Evaluation. *2.7.1. Bacterial Culture S. aureus.* ATCC 25923 was cultured in TSB at 37 °C for 8 h. The bacteria were then collected and washed three times with sterile saline to obtain a bacterial suspension for further use.

2.7.2. Induction of Persisters. A 100 μL aliquot of the prepared *S. aureus* suspension was inoculated into 100 mL of MHB and incubated at 37 °C for 12 h. Afterward, 40 mL of the culture was supplemented with vancomycin (Van, 50 μg/mL) and incubated for an additional 8 h to induce persister formation. The culture was then centrifuged at 7500 rpm for 3 min to enrich persistent *S. aureus*, followed by three washes with saline.

2.7.3. Minimum Inhibitory Concentration (MIC). The MIC values were determined by serial dilution of the compounds in a 96-well plate containing 100 μL of broth per well. Briefly, exponentially growing *S. aureus* cultures were diluted to 10^6 CFU/mL and added to each well containing serial 2-fold dilutions of antibiotics. Plates were incubated at 37 °C for 24 h. MIC was defined as the lowest concentration at which no visible bacterial growth was observed, as determined by measuring optical density (OD) at 600 nm. Wells containing bacteria without antibiotics served as positive controls, while wells without bacteria served as negative controls. All assays were performed in triplicate.

2.7.4. Biphasic Killing Kinetics of Persisters. A 100 μL aliquot of *S. aureus* suspension was inoculated into 100 mL of MHB and incubated at 37 °C for 12 h. Then, 0.4 mL of the culture was transferred to 40 mL of fresh MHB containing Van at 50 × MIC (50 μg/mL) to induce persister formation. This point was marked as 0 h. Samples were

https://doi.org/10.1021/acsami.5c11777
ACS Appl. Mater. Interfaces XXXX, XXX, XXX−XXX

Table 1. MIC and MBC with Different Mechanisms of Action (*S. aureus* ATCC 25923)

Mechanism of action	Name	Classification	MIC	MBC
Cell wall synthesis inhibitors	Meropenem (Mer)	β-lactams	65 ng/mL	2 μg/mL
	Vancomycin (Van)	Glycopeptides	1 μg/mL	8 μg/mL
	Amoxicillin (Amo)	β-lactams	125 ng/mL	125 ng/mL
Cell membrane disruptors	Polymyxin B (PMB)	Polypeptides	64 μg/mL	256 μg/mL
Protein synthesis inhibitors	Gentamicin (Gen)	Aminoglycosides	1 μg/mL	16 μg/mL
	Tobramycin (Tob)	Aminoglycosides	250 ng/mL	16 μg/mL
	Clarithromycin (Cla)	Macrolides	65 ng/mL	0.5 μg/mL
	Tetracycline (Tet)	Tetracyclines	65 ng/mL	1 μg/mL
Nucleic acid synthesis inhibitors	Rifampicin (Rif)	Rifamycins	8 ng/mL	63 ng/mL
	Moxifloxacin (Mox)	Fluoroquinolones	4 ng/mL	32 ng/mL
	Sitafloxacin (Sit)	Fluoroquinolones	16 ng/mL	64 ng/mL

collected at 2, 4, 6, 8, 10, 12, and 24 h post-treatment, serially diluted, and plated for colony counting.

2.7.5. Antibacterial Evaluation of NPs against Persisters. In 96-well plates, 80 μL of M9 medium and 20 μL of the NPs (corresponding to a final antibiotic concentration of 10 × MIC) were added to each well, followed by 100 μL of the persisters suspension. Plates were incubated at 37 °C for 24 h, then serially diluted and plated to determine bacterial viability.

2.7.6. Evaluation of the Antibacterial Effects of Antibiotics and the Drug-Loaded NPs under Oxidative Stress Conditions. Hydrogen peroxide was added to the wells of a 96-well plate to mimic the oxidative stress conditions of the intracellular environment. Antibiotics or NPs were subsequently added to the designated wells. After 24 h of incubation, cultures were centrifuged and plated for viable colony counts.

2.7.7. Evaluation of the Antibacterial Effects of Antibiotics and the Drug-Loaded NPs under Acidic Conditions. To simulate the acidic conditions within host cells, PBS buffer at pH 5.5 was added to 96-well plates. Antibiotics or the NPs were introduced into the respective wells, followed by incubation at 37 °C for 24 h. Cultures were then centrifuged and plated for CFU enumeration.

2.7.8. Construction and Cultivation of Green Fluorescent Protein (GFP)- Escherichia coli (E. coli). *E. coli* BL21 was first cultured, and the *pBAD* plasmid was extracted. The GFP gene fragment was then integrated, followed by transformation through ice-bath incubation, heat shock, and recovery culture. The transformed bacteria were plated onto LB agar containing ampicillin to select positive clones, which were further cultured and verified. The bacteria were further cultured, with GFP expression induced by arabinose under *araBAD* promoter regulation. After the resulting GFP-*E. coli* was treated with Van for 8 h to generate GFP-labeled persisters, which were then washed and analyzed for fluorescence intensity by flow cytometry.

2.8. Intracellular Antibacterial Evaluation. *2.8.1. Cell Culture.* Raw 264.7 macrophages were maintained in DMEM supplemented with 10% FBS and 1% penicillin-streptomycin. Cells were incubated at 37 °C in a humidified 5% CO_2 atmosphere, with medium replacement every other day.

2.8.2. Establishment of Intracellular Persisters. Raw 264.7 cells were seeded at a density of 1×10^5 cells per well and allowed to adhere for 18−24 h. Subsequently, *S. aureus* was added at a multiplicity of infection of 10. After 1 h of infection, cells were washed three times with PBS and treated with 50 μg/mL gentamicin (Gen) for 1 h to eliminate extracellular bacteria. Then, 50 μg/mL Van was added and incubated for 24 h to induce intracellular persisters.

2.8.3. Antibacterial Assessment against Intracellular Persisters. After infection and persistence induction, Raw 264.7 macrophages were washed three times with PBS and treated with either free antibiotics or NPs for 24 h. Following treatment, cells were lysed using 0.1% (v/v) Triton X-100 in PBS. The released intracellular *S. aureus* was serially diluted and plated in triplicate on TSA agar. Colonies were enumerated after overnight incubation to assess bacterial survival.

2.8.4. Cellular Uptake of the NPs. Raw 264.7 macrophages were seeded into confocal dishes at a density of 3×10^5 cells/mL for CLSM imaging. NR@F(AM) NPs (10 μg/mL, calculated based on NR content) and mannose-free NR@FA NPs were added to the culture medium. After incubation for varying durations, nanoparticle internalization was visualized using CLSM, and cellular fluorescence intensity was quantified using ImageJ software.

2.8.5. Cellular Uptake of PMB. Equal amounts of PMB and FITC were dissolved in water and reacted for 24 h, followed by dialysis to purify the resulting compound PMB-FITC. The preparation of PMB-FITC@F(AM) was performed as described in Section 2.3. Subsequently, equal amounts of PMB-FITC and PMB-FITC@F(AM) (based on PMB-FITC mass) were incubated with cells for different durations (1, 3, 6, 12, and 24 h), finally fluorescence intensity was measured by flow cytometry.

2.9. Protein Leakage Assay. Planktonic persistent *S. aureus* are incubated with either free antibiotics or the NPs for 24 h. After treatment, bacterial cells were lysed using RIPA lysis buffer. The concentration of released proteins in the supernatant was then quantified using a BCA protein assay kit.

2.10. Quantification of Local Rif Concentration. *2.10.1. Planktonic Rif Concentration.* *S. aureus* was incubated with free Rif or Rif@F(AM) NPs in 96-well plates. After incubation, the extracellular concentration of Rif was measured using a Rif concentration assay kit.

2.10.2. Intracellular Rif Concentration. After the establishment of intracellular *S. aureus* persisters, cells were treated with either free Rif or Rif@F(AM) NPs. Intracellular concentration of Rif was quantified using the same Rif assay kit.

2.11. Proton Motive Force Assay. *S. aureus* treated with or without CCCP were diluted and counted after coincubation with the same concentrations of antibiotics and NPs.

2.12. In Vivo Animal Studies. *2.12.1. Mice Handling.* Female BALB/c mice were purchased from Charles River Laboratories. All animal care and experimental procedures were conducted in strict accordance with the *Guide for the Care and Use of Laboratory Animals* published by the National Research Council. All animal experiments were reviewed and approved by the institutional animal ethics committee, and were conducted under the supervision of Beijing Yongxinkangtai Technology Development Co., Ltd. (Approval No. YxkT2025L018).

2.12.2. In Vivo Antibacterial Evaluation (Peritonitis Model). An intraperitoneal infection model of *S. aureus* persisters was established to evaluate the *in vivo* antibacterial efficacy (n = 3 per group, and three experimental groups were established: a control group (Con), a free Sit treatment group (Sit), and a Sit@F(AM) treatment group (Sit@F(AM)). Briefly, mice were intraperitoneally injected with *S. aureus* (10^8 CFU in 100 μL). After 6 h, Van (75 mg/kg) was administered to induce a persistent bacterial state. At 16 h postinfection, the persistent peritonitis model was considered established. Mice were then treated with either free Sit or Sit@F(AM) NPs via intraperitoneal injection at an equivalent dose of 2 mg/kg (100 μL). After 24 h of treatment, the mice were euthanized, and 2 mL of HBSS was injected into the peritoneal cavity to collect the peritoneal lavage fluid. Half of the peritoneal lavage fluid was centrifuged, and the supernatant was collected to quantify extracellular CFU. The remaining half was incubated with lysozyme

https://doi.org/10.1021/acsami.5c11777
ACS Appl. Mater. Interfaces XXXX, XXX, XXX−XXX

(15 μg/mL) to eliminate extracellular bacteria, followed by lysis with HBSS containing 0.1% Triton X-100 to quantify intracellular CFU.

2.13. Statistical Analysis Methods. All experiments in this study were independently repeated at least three times unless otherwise stated. Experimental data are presented as mean ± standard deviation (mean ± SD). Tukey's test was used for multiple group comparisons, and *t* test was used for two-group comparisons to evaluate the statistical significance of differences between groups. A *p*-value of less than 0.05 was considered statistically significant, with significance levels indicated as follows: $*p < 0.05$, $**p < 0.01$, $***p < 0.001$, $****p < 0.0001$, and ns (not significant, $p > 0.05$).

3. RESULTS AND DISCUSSION

3.1. Evaluation of Antibiotics with Different Mechanisms of Action against *S. aureus*. Our previous review systematically summarized and categorized strategies to eradicate persistence, and discussed the roles and potential of different antibiotics in clearing persistent bacteria. Drugs with distinct mechanisms may have significantly different effects on persistent bacteria.[26] Therefore, we selected four classes of antibiotics with distinct modes of action, including (i) cell wall synthesis inhibitors (e.g., β-lactams, Meropenem (Mer)), (ii) membrane disruptors (e.g., polymyxins, PMB), (iii) protein synthesis inhibitors (e.g., aminoglycosides, Gen), and (iv) nucleic acid synthesis inhibitors (e.g., fluoroquinolones, Sit). MIC and MBC of these antibiotics against *S. aureus* (Table 1) were first determined to assess their bactericidal activities. The results indicated that among the cell wall synthesis inhibitors, amoxicillin (Amo) exhibited both low MIC and MBC values (125 ng/mL), demonstrating consistent bactericidal activity. In contrast, Mer showed a lower MIC (65 ng/mL) but a significantly higher MBC (2 μg/mL), suggesting a predominantly bacteriostatic effect. For the protein synthesis inhibitors, the macrolide clarithromycin (Cla) showed low MIC (65 ng/mL) and MBC (0.5 μg/mL), potentially due to its ability to block the ribosomal elongation phase. Tobramycin (Tob), with an MBC as high as 16 μg/mL, displayed diminished efficacy against persistent bacteria, likely due to its uptake being energy-dependent. Among the nucleic acid synthesis inhibitors, Sit, Rif, and moxifloxacin (Mox) all demonstrated low MIC values (16, 8, and 4 ng/mL, respectively). These antibiotics exert their effects by inhibiting DNA gyrase or RNA polymerase, thereby blocking core genetic transcription processes, and are generally effective in disrupting the physiological functions of bacteria regardless of their metabolic state. In contrast, cell membrane disruptors of PMB, primarily targets lipopolysaccharides in the outer membrane of Gram-negative bacteria. As a result, it exhibited substantially higher MIC (64 μg/mL) and MBC (256 μg/mL) values against Gram-positive *S. aureus*. Given the diverse antimicrobial potencies observed, a standardized concentration equivalent to 10 × MIC was used for all antibiotics in the subsequent bactericidal evaluations.

3.2. Establishment of Planktonic *S. aureus* Persister Model and Evaluation of Antibiotic Efficacy of Antibiotics. To induce the formation of planktonic persisters (Figure 1a), *S. aureus* was incubated in MHB for 12 h to reach a stationary phase, during which nutrient depletion and accumulation of metabolic byproducts reduced bacterial activity and increased resistance to environmental stress. Subsequently, 50 μg/mL of Van was added to eliminate actively growing bacteria and induced persisters.[16,50] During this process, bacterial killing kinetics revealed that Van rapidly eliminated sensitive bacteria within the first 6 h, resulting in a

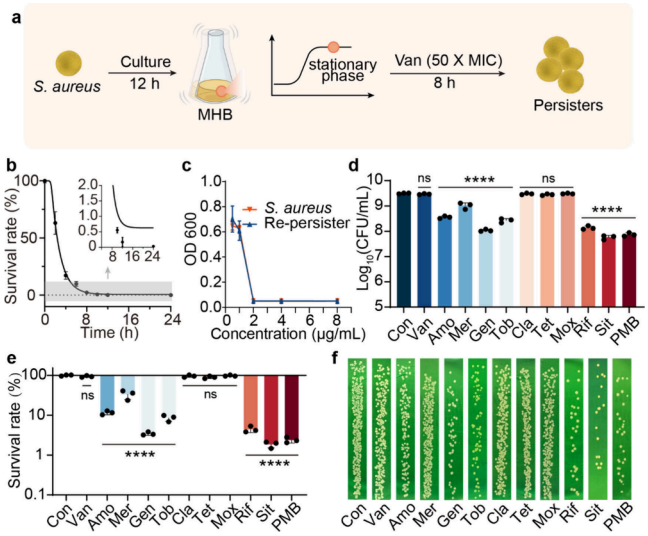

Figure 1. Validation of planktonic persister construction and antibiotic efficacy. (a) Schematic of planktonic persisters induction stationary-phase *S. aureus* to 50 × MIC Van for 8 h. (b) Biphasic killing curve of planktonic persisters, with bacterial counts decreasing from to 10^9 CFU and plateauing below 1%, consistent with the characteristic biphasic killing profile of persisters. (c) Comparison of Van MIC values between sensitive *S. aureus* and resuscitated persisters, showing consistent MICs, indicating no development of resistance. (d–f) Antibacterial evaluation of antibiotics with distinct mechanisms, showing survival rates and representative colony morphologies. $n = 3$, data are expressed as the mean ± SD. Tukey's test, $****p < 0.0001$.

sharp decline in bacterial count. However, after 8 h of treatment, the bacteria number plateaued at approximately 1% (Figure 1b), exhibiting a biphasic killing curve characteristic of persister subpopulations.[51] To clarify the nongrowth characteristics of persistent bacteria, an GFP-*E. coli* strain was constructed (Figure S1). GFP-*E. coli* exhibited strong green fluorescence when induced with arabinose, whereas in the absence of arabinose, the fluorescence gradually diminished as the bacteria proliferated. By 12 h, the fluorescence was almost undetectable. Conversely, Van-induced persistent GFP-*E. coli* maintained high fluorescence, indicating the nongrowth property of the persisters (Figure S1). To further confirm the distinction between persisters and resistant bacteria, the isolated persistent *S. aureus* were reinoculated into fresh medium, where they resumed normal growth and exhibited MIC values identical to those of drug-sensitive *S. aureus* (Figure 1c). Moreover, the subpopulation of *S. aureus* persisters remained unchanged upon treatment with 10 × MIC Van, with no further expansion observed (Figure S2). This confirms that these bacteria did not possess genetic resistance.

Subsequently, we conducted bactericidal studies on persisters using a range of antibiotics. Cell wall synthesis inhibitors generally showed limited efficacy. Mer and Amo eliminated 70–90% of persisters (Figure 1d-f), yet overall bactericidal activity remained modest. In contrast, protein synthesis inhibitors showed marked variability in their ability to eliminate persisters. The macrolide antibiotic Cla and the tetracycline antibiotic Tet exhibited no discernible bactericidal activity against persistent *S. aureus*. By contrast, the aminoglycoside antibiotics Gen and Tob, which are commonly used to target Gram-negative bacteria, exhibited potent bactericidal

https://doi.org/10.1021/acsami.5c11777
ACS Appl. Mater. Interfaces XXXX, XXX, XXX–XXX

activity against persisters, eliminating over 90% of the persistent subpopulation, with survival rates of 4% and 9%, respectively. Among nucleic acid synthesis inhibitors, the fluoroquinolone Mox exhibited limited activity. However, Sit is another fluoroquinolone, showed the most potent killing effect, reducing the persisters population to below 2%. Rif is a first-line antituberculosis agent that blocks RNA synthesis by targeting bacterial DNA-dependent RNA polymerase, also demonstrated strong bactericidal activity, achieving a 96% killing rate (Figure 1e). While antibiotic efficacy varied, the data collectively suggest that inhibitors of cell wall synthesis are less effective against persisters. This is likely because persisters are in a nondividing state, with reduced cell wall synthesis and division rates, and may also activate cell wall stress responses (CWSS),[52,53] reinforcing their structural integrity. Importantly, bacterial persistence does not equate to dormancy. Instead, central carbon metabolism is reprogrammed,[25] while nucleic acid and protein synthesis remain active. Thus, inhibitors targeting these pathways exert greater efficacy against persisters.[54] Notably, PMB is a cyclic peptide that disrupts bacterial membranes and is primarily used against Gram-negative pathogens, exhibited strong bactericidal activity against *S. aureus* persisters as well. By targeting the bacterial membrane regardless of metabolic state, PMB reduced bacterial survival to 3%, comparable to the effects of Sit and Rif. Therefore, Gen, Sit, Rif, and PMB emerged as the most promising candidates for targeting planktonic persisters.

3.3. Establishment of Intracellular S. aureus Persister Model and Evaluation of Antibiotic Efficacy of Antibiotics. To further investigate the efficacy of antibiotics against persisters in the intracellular environment, we extended the planktonic persister model to establish an intracellular persistent *S. aureus* infection model in macrophages. Specifically, Raw 264.7 macrophages were infected with *S. aureus* (Figure 2a), and extracellular planktonic bacteria were removed by Gen treatment.[55] The infected macrophages were then incubated in culture medium containing 50 μg/mL Van for 24 h to induce intracellular persisters.[56,57] During this period, a characteristic biphasic killing curve was also observed. Bacterial counts dropped sharply within the first 6 h and then plateaued, with approximately 65% of bacteria surviving (Figure 2b), consistent with features of intracellular persisters.[25]

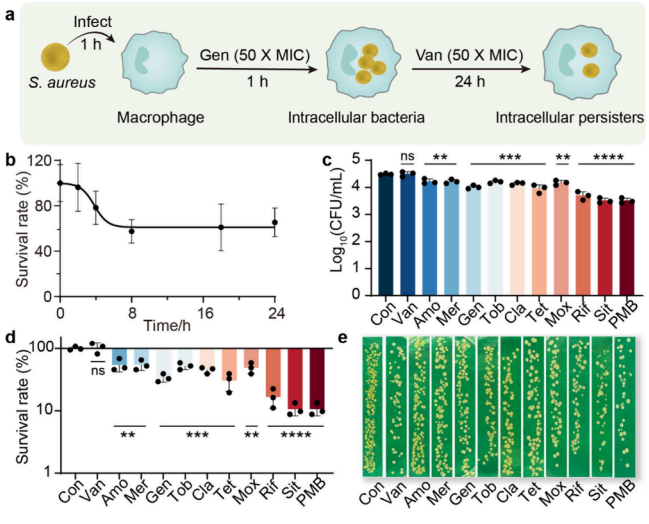

Figure 2. Establishment of intracellular persister construction and antibiotic screening. (a) Schematic of intracellular persisters, intracellular persisters generated by infecting Raw 264.7 macrophages with *S. aureus*, followed by Van treatment (50 × MIC, 24 h). (b) Intracellular persisters exhibited a biphasic killing curve similar to that of planktonic persisters. (c–e) Antibacterial evaluation of antibiotics with distinct mechanisms, showing survival rates and representative colony morphologies. $n = 3$, data are expressed as the mean ± SD t test, ****$p < 0.0001$, ***$p < 0.001$, **$p < 0.01$, $^{ns}p > 0.05$.

Then, the bactericidal efficacy of the antibiotics against intracellular persisters was evaluated. Consistent with observations in the planktonic model, antibiotics targeting cell wall synthesis inhibitors exhibited the weakest activity, with killing rates not exceeding 46%. Protein synthesis inhibitors showed moderate activity, with maximal killing rates under 70%. In contrast, nucleic acid synthesis inhibitors displayed superior efficacy, with Sit achieving the highest bactericidal activity, eliminating 90% of intracellular persisters (Figure 2c-e). Compared to planktonic conditions, the intracellular environment is generally less favorable for the survival of most bacteria, but except for a few that have evolved mechanisms to thrive within host cells. Additionally, it provides additional protective barriers, such as the host cell membrane, acidic pH, and oxidative stress, that significantly influence antibiotic uptake and stability. As a result, antibiotic clearance within host cells is typically reduced. For example, Gen possesses multiple surface cationic groups and exhibits strong electrostatic interactions with host cell membranes under physiological conditions, thereby limiting its intracellular uptake. Consequently, the survival rate of intracellular persisters (~34%) was markedly higher than that of planktonic persisters (~3%) (Figure 2d, 2e). Similarly, the eradication efficacy of Tob against intracellular persisters also declined to below 90%. Interestingly, Cla and Tet demonstrated improved activity in the intracellular model, with killing rates of 55% and 70%, respectively, compared to their negligible effects against planktonic persisters. However, this apparent increase may be partially reflected differences in the initial bacterial burden between the two models. In contrast, Sit and Rif demonstrated strong bactericidal activity against persisters in both planktonic and intracellular models, achieving killing rates of ~98% and ~96% in the planktonic setting, and slightly reduced yet substantial rates of ~89% and ~83% in the intracellular environment. This relatively preserved intracellular efficacy may be attributed to their lipophilic nature, which allows passive diffusion across host cell membranes and reversible binding to intracellular proteins.[58,59] Consistently, PMB also exhibited strong bactericidal activity against intracellular persisters, owing to its potent membrane-penetrating capability. Nonetheless, a portion of these antibiotics still accumulates within acidic lysosomes, limiting their cytosolic availability.[60] In addition, the acidic and enzyme-rich intracellular milieu poses additional challenges by potentially compromising drug stability and activity.

3.4. Preparation and Characterization of Antibiotic Loaded F(AM) NPs. The results above suggest that intracellular pharmacokinetics and pharmacodynamics play a critical role in shaping the bactericidal performance of antibiotics. Based on this, we hypothesized that if the limitations of cellular uptake and intracellular microenvironment could be circumvented, thereby allowing antibiotics to act directly on the persisters, the clearance efficiency against intracellular persisters might be further improved. Accordingly, a targeted drug delivery platform based on poly(α-*N*-acryloyl-

https://doi.org/10.1021/acsami.5c11777
ACS Appl. Mater. Interfaces XXXX, XXX, XXX−XXX

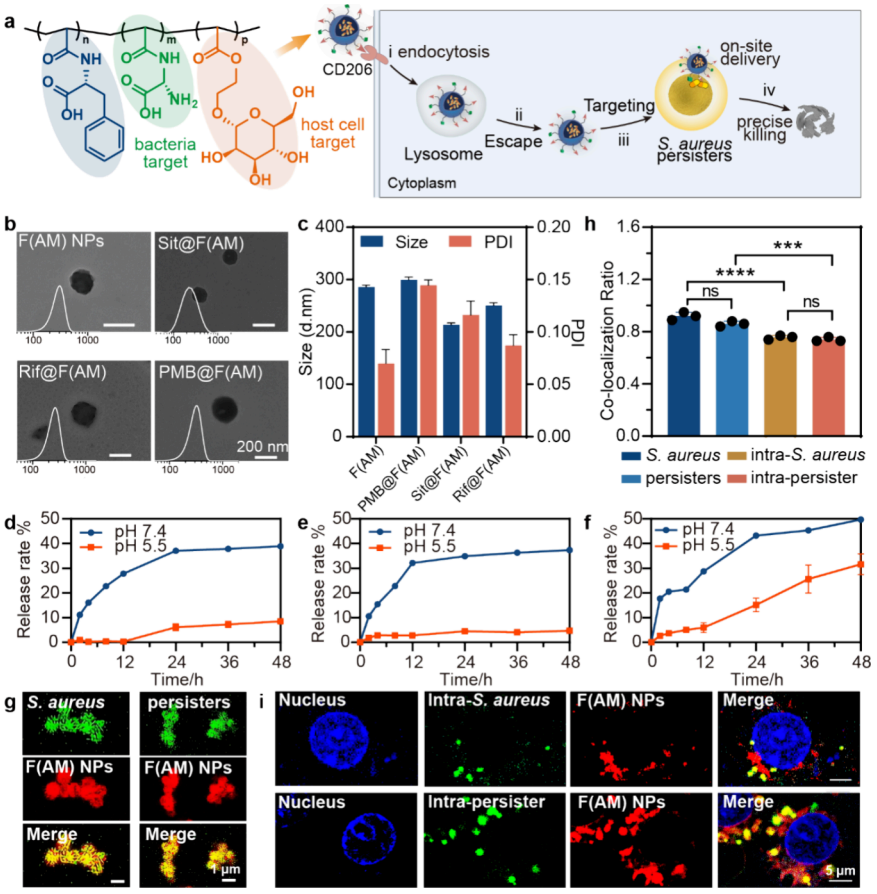

Figure 3. Characterization and specific targeting performance of F(AM). (a) F(AM) exhibits specific bacterial and cellular targeting. Following self-assembly, F(AM) enters cells via mannose-mediated targeting and escapes from lysosomes. It then specifically targets intracellular bacteria and releases antibiotics on-site to eradicate intracellular persisters. (b) TEM images and size distributions of F(AM), PMB@F(AM), Sit@F(AM), and Rif@F(AM) NPs. (c) Particle size and PDI of F(AM), PMB@F(AM), Sit@F(AM), and Rif@F(AM) NPs. (d) Cumulative drug release of Sit@F(AM) in pH 7.4 and pH 5.5. (e) Cumulative drug release of Rif@F(AM) in pH 7.4 and pH 5.5. (f) Cumulative drug release of PMB@F(AM) in pH 7.4 and pH 5.5. (g) Confocal images showing colocalization of F(AM) with sensitive and planktonic persistent. Strong fluorescence overlapped between FITC-labeled *S. aureus* and NR@F(AM) indicates effective bacterial targeting by F(AM). (h) PCC values from fluorescence colocalization analysis of F(AM) targeting different bacterial types. (i) Confocal images showing colocalization of F(AM) with intracellular and intracellular. The strong overlap of FITC-labeled *S. aureus* with NR@F(AM) fluorescence suggests that F(AM) also effectively targets intracellular persistent *S. aureus*. $n = 3$, data are expressed as the mean ± SD. Tukey's test, $^{****}p < 0.0001$, $^{***}p < 0.001$, $^{ns}p > 0.05$.

phenylalanine)-*block*-poly(*β*-*N*-acryloyl-D-aminoalanine-*co*-2-*O*-acetyl-*α*-D-mannosyloxy) (F(AM)) was designed to enable cascade targeting of host cells and intracellular bacteria, achieving on-site antibiotic delivery at the bacterial niche. F(AM) is a copolymer synthesized via PET-RAFT polymerization (Scheme S1, Figures S3−S7 and Table S1). The resulting NPs possess free mannose and D-aminoalanine groups on their surface, enabling specific cellular uptake via mannose ligand−receptor recognition. Upon internalization, the NPs escape lysosomal entrapment via the proton sponge effect. Meanwhile, the surface-exposed D-aminoalanine targets intracellular bacteria by inserting into the peptidoglycan, thereby facilitating localized antibiotic delivery (Figure 3a). Sit, Rif, and PMB were then chosen to loaded into the F(AM) NPs in a water/DMSO (9:1, v/v) solvent system to form Sit@F(AM), Rif@F(AM), and PMB@F(AM) NPs. TEM revealed that the NPs were uniformly spherical (Figure 3b) with diameters under 300 nm. The polydispersity index (PDI) confirmed uniform particle dispersion (Figure 3c), while stable surface potentials (Figure S8) further demonstrated the favorable colloidal stability and drug-carrying capacity of the F(AM) NPs (Figure 3b, c). Additionally, these NPs exhibited good cell compatibility (Figure S9).

Sit and Rif are lipophilic antibiotics predominantly composed of hydrophobic heterocycles. Their encapsulation within F(AM) NPs is primarily driven by hydrophobic interactions with the core of the nanostructure. Sit@F(AM) exhibited the DLC of 6.6% and the DLE of 72.7%, while Rif@F(AM) achieved a higher DLC of 13.6% with the DLE of 81.6% (Figure S10, Table S2). PMB, a hydrophilic cationic peptide rich in amino and guanidinium groups, interacted strongly with the negative charge of F(AM) via hydrogen bonding and electrostatic interactions. Owing to this interaction, PMB@F(AM) achieved a notably high DLC of 17.3% and the DLE of 75.0%, significantly outperforming Sit and Rif (Table S2). Drug release profiles under pH 7.4 demonstrated that Sit@F(AM) showed a slightly lower cumulative release of 37%, consistent with its stronger retention within the hydrophobic matrix (Figure 3d). In contrast, Rif@F(AM) exhibited a cumulative release of 39% over 48 h, indicative of favorable sustained-release behavior (Figure 3e). At pH 5.5, the cumulative release of Sit@F(AM) over 48 h was markedly reduced to ∼4.5%, while Rif@F(AM)

https://doi.org/10.1021/acsami.5c11777
ACS Appl. Mater. Interfaces XXXX, XXX, XXX−XXX

showed a release of ~ 8.5%, indicating high drug retention under acidic conditions. PMB underwent rapid release from the NPs and showed substantial drug release under acidic conditions (Figure 3f). Its release rate was notably faster than those of Sit and Rif.

3.5. Targeting Ability of F(AM) NPs to Planktonic Persisters and Intracellular Persisters. Previous studies have shown that the bacterial targeting ability of aminoalanine-based polymers correlates with bacterial viability.[61] To evaluate the targeting capacity of the F(AM) toward planktonic and intracellular persisters, we employed CLSM to assess the colocalization between F(AM) NPs and persistent *S. aureus*. As shown in Figure 3g, NR@F(AM) NPs loaded with the fluorescent probe NR exhibited strong colocalization with the sensitive *S. aureus* labeled by FITC in a pronounced yellow fluorescence signal. The Pearson correlation coefficient (PCC) was up to 0.92 (Figure 3h), indicating that F(AM) has excellent recognition and targeting ability for sensitive bacteria. Interestingly, CLSM images also revealed a strong colocalization between the red-fluorescent NR@F(AM) NPs and the green-fluorescent FITC-labeled persistent bacteria (Figure 3g), with a high PCC of 0.86 (Figure 3h). Although the targeting efficiency toward persisters was slightly lower than that for sensitive bacteria, this difference may stem from the reduced activity of peptidoglycan-binding protein 4 (PBP4) proteins on the surface of persistent bacterial membranes, which could impair the binding of NPs.[61] The difference between these two PCC values was minimal and not statistically significant, with both exceeding 0.6, indicating that F(AM) demonstrates strong targeting specificity toward planktonic persisters.

Subsequently, the targeting performance of F(AM) toward intracellular persisters was investigated. The cellular uptake rate of F(AM) is one of the key factors influencing their targeting efficiency. The mannose ligand/receptor-specific recognition on the surface of F(AM) NPs enables their entry into host cells. To validate the macrophage-targeting ability of F(AM) NPs, NR was loaded into F(AM) NPs to monitor their cellular internalization efficiency. NR@FA NPs, which lack mannose moieties, were used as controls. Phagocytosis assays demonstrated that NR@F(AM) NPs were taken up by macrophages more efficiently than NR@FA NPs. Fluorescence imaging revealed their clear cytoplasmic localization, with markedly stronger signals at both 0.5 and 3 h (Figures S11, S12), indicating that F(AM) NPs rapidly crossed the cell membrane and achieved efficient internalization via mannose receptor-mediated targeting. We hypothesize that the rapid penetration of F(AM) facilitates the targeting of intracellular persisters. After coincubation of NR@F(AM) NPs with FITC-labeled *S. aureus*-infected Raw 264.7 macrophages, the red fluorescence signal of NR@F(AM) NPs within the host cells showed substantial overlap with the green fluorescence of sensitive FITC-*S. aureus*, with a PCC of approximately 0.76 (Figure 3h). This indicates that F(AM) NPs are capable of rapidly penetrating the cell membrane and effectively recognizing and targeting intracellular *S. aureus* (Figure 3i). The targeting efficiency for intracellular bacteria (PCC = 0.76) was slightly lower than that for planktonic bacteria (PCC = 0.92), likely due to interference from intracellular proteins and subcellular structures with the interaction between NR@F(AM) NPs and bacteria. In addition, the harsh intracellular microenvironment may suppress bacterial metabolism and reduce viability, further weakening the colocalization. For intracellular persisters, NR@F(AM) NPs also exhibited strong colocalization, with a PCC of approximately 0.73 comparable to that observed for intracellular *S. aureus*, yet significantly lower than that for planktonic persisters. These results indicate that NR@F(AM) NPs possess effective targeting capability toward intracellular persisters. Notably, the targeting behavior of F(AM) NPs appeared to correlate with bacterial viability. Persisters in planktonic and intracellular forms exhibit differences in metabolic pathways and activity due to their distinct ecological niches,[12,62] which in turn influence the targeting performance of F(AM) NPs.

3.6. Evaluation of Antimicrobial Performance of NPs against Planktonic Persisters. Preserving the antimicrobial activity of an antibiotic after it is loading into F(AM) is essential for maintaining its bactericidal or bacteriostatic effect. To evaluate the antibacterial efficacy of F(AM) after loading different antibiotics, we measured the MIC and MBC of Sit@F(AM), Rif@F(AM), and PMB@F(AM) NPs (Figure 4a, 4b

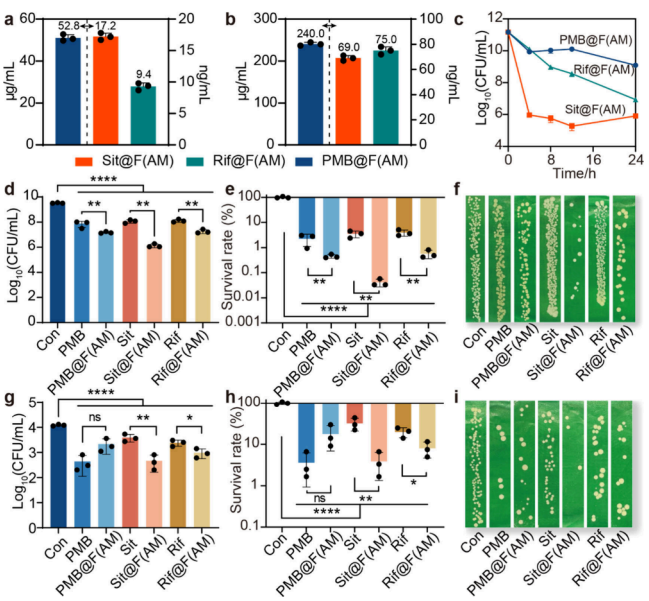

Figure 4. Antibacterial evaluation of F(AM)-loaded NPs against planktonic and intracellular peisisters. (a) MIC and (b) MBC of Sit@F(AM), Rif@F(AM) and PMB@F(AM) NPs against *S. aureus*. (c) Time-kill kinetics of three antibiotic-loaded NPs against *S. aureus*. (d–f) Antibacterial activity of three antibiotic-loaded NPs against planktonic persisters, assessed by CFU counts, survival rates and representative colony morphologies. (g–i) Antibacterial activity of three antibiotic-loaded NPs against intracellular persisters, assessed by CFU counts, survival rates and representative colony morphologies. $n = 3$, data are expressed as the mean ± SD. Tukey's test, $^{****}p < 0.0001$, $^{**}p < 0.01$, $^{*}p < 0.05$, $^{ns}p > 0.05$.

and Figure S13). The MICs were 17.2 ng/mL for Sit@F(AM), 9.4 ng/mL for Rif@F(AM), and 52.8 μg/mL for PMB@F(AM) (Figure 4a), which were generally consistent with those of the free antibiotics. These findings indicate that the F(AM) enables antibiotics encapsulation and sustained release without compromising the intrinsic antibacterial activity of the antibiotics, primarily serving as a carrier for controlled release and precise delivery. Interestingly, although the three antibiotics exhibited distinct release profiles (Figure 3c), with Sit releasing most slowly, PMB most rapidly, and Rif at an intermediate rate. This outcome likely reflects the interplay between the unique bactericidal mechanism of each antibiotic and the targeted delivery provided by the F(AM). To further

https://doi.org/10.1021/acsami.5c11777
ACS Appl. Mater. Interfaces XXXX, XXX, XXX–XXX

explore this, bactericidal kinetics of these three drug-loaded NPs was assessed. For *S. aureus*, Sit@F(AM) achieved the most rapid bacterial clearance despite, potentially due to the bactericidal mechanism of Sit targeting DNA replication, which may allow for early phase action. In contrast, PMB@F(AM) exhibited weaker initial bactericidal activity, possibly because the sustained-release behavior delayed its typical membrane-disruptive effect. The release rate and bactericidal ability of Rif@F(AM) are both intermediate. This may be related to its specific inhibition of bacterial DNA-dependent RNA polymerase, which hinders the synthesis of mRNA and thus inhibits the synthesis of bacterial nucleic acids. Notably, despite the marked differences in release profiles among the three NPs, their overall antibacterial activity remained unaffected. This finding points to a more complex underlying phenomenon. The release rate is not the sole determinant of bactericidal efficacy, but is likely intertwined with the mechanism of action of the antibiotics and the ecological niche of the target bacteria.

Given the drug delivery and targeting capabilities of F(AM), we further investigated whether it could enhance the bactericidal efficacy of the antibiotics against planktonic persisters (Figure 4d-f). Taking Rif as an example, free Rif achieved a bacterial killing rate of approximately 96% against planktonic persisters, whereas Rif@F(AM) reduced the bacterial load from 10^9 CFU to 10^7 CFU, reaching a killing rate of 99.4%. This potentiation may be due to the targeted release of Rif upon Rif@F(AM) binding to bacteria. Similarly, PMB@F(AM) exhibited a moderate improvement in bactericidal activity. Compared to free PMB, which achieved a ∼ 98% killing rate, PMB@F(AM) increased the kill efficacy to about 99.6%. Notably, Sit@F(AM) demonstrated the most potent clearance capability, reducing bacterial counts from 10^9 CFU to below 10^6 CFU and achieving a killing rate of 99.96%. This is significantly higher than that of ∼ 96% observed with free Sit, indicating exceptional bactericidal potential. Persistent bacteria maintain active transcription but exhibit defective translation. As Sit targets DNA gyrase, it can rapidly disrupt DNA function in persisters, leading to irreversible damage.

3.7. Evaluation of Antimicrobial Performance of NPs against Intracellular Persisters. Persistent bacterial populations inhabit a range of ecological niches within the host, transitioning from planktonic states to intracellular compartments, accompanied by corresponding shifts in survival strategies, metabolic activity, and antibiotic susceptibility. Compared to their planktonic counterparts, intracellular bacteria benefit from both physical shielding and metabolic refuge, rendering them significantly more resistant to eradication. This highlights the critical need to target intracellular persisters. Accordingly, we assessed the intracellular antibacterial efficacy of Sit@F(AM), Rif@F(AM), and PMB@F(AM) formulations (Figure 4 g-i).

Both Rif@F(AM) and Sit@F(AM) significantly reduced the intracellular populations of persisters. Rif@F(AM) lowered the survival rate of intracellular persisters from ∼20% (with free Rif treatment) to ∼8%. Notably, Sit@F(AM) reduced bacterial survival from 32% (with free Sit treatment) to below 4% (Figure 4h). While these results suggest that the F(AM) NPs can enhance the intracellular bactericidal activity of antibiotics, a pronounced difference remains between intracellular and extracellular clearance. For example, Sit@F(AM) reduced planktonic persisters survival to just 0.04% (Figure 4e), effectively achieving near-complete eradication, whereas intracellular survival remained around 4%. This discrepancy likely results from host-cell barriers limiting the intracellular concentration of delivered antibiotics. The fact that free Sit reduced planktonic persisters survival to approximately 4%, a level lower than that observed intracellularly, further underscores the protective role of the host environment.

In contrast, PMB@F(AM) did not exhibit improved intracellular killing over free PMB; in fact, its efficacy was even lower, contrasting with the results observed in planktonic settings. This may be due to differing intracellular delivery pathways. Free PMB may diffuse or be actively transported into cells,[63] whereas PMB@F(AM) must undergo uptake, endocytosis, and intracellular trafficking, the processes that can reduce delivery efficiency. To verify this view, cellular internalization efficiency of PMB and PMB@F(AM) was investigated. PMB was conjugated with FITC to form the PMB-FITC compound. Equal amounts of PMB-FITC and PMB-FITC@F(AM) (based on PMB-FITC mass) were incubated with cells for various durations to evaluate their cellular uptake efficiency. At the first 6 h, PMB-FITC showed an increasing uptake trend, outperforming PMB-FITC@F(AM). Beyond 6 h, the fluorescence intensity of PMB-FITC gradually declined and eventually dropped below that of PMB-FITC@F(AM). The latter maintained consistently higher fluorescence, indicating superior intracellular accumulation over time (Figure S14). This result indicates that PMB acts by rapidly disrupting bacterial membranes, even though this comes at the cost of host cell damage, thereby making it best suited for a "high-concentration, short-duration" burst delivery strategy. The sustained-release properties of F(AM) help maintain prolonged drug levels but may delay the onset of PMB action during critical early treatment stages, reducing its ability to rapidly eliminate intracellular persisters.

3.8. *In Vivo* Antibacterial Evaluation of Sit@F(AM) against Intracellular Persisters. Sit@F(AM) exhibited superior efficacy in eradicating both planktonic and intracellular persisters. To further assess its targeted antibacterial performance under physiologically relevant conditions, we established a peritoneal infection model (Figure 5a). Mice were intraperitoneally infected with *S. aureus* and subsequently treated with Van to induce persisters formation.[57,64] At 24 h postinduction, mice received either free Sit or Sit@F(AM) (both at a Sit-equivalent dose of 2 mg/kg), and peritoneal lavage was collected to quantify extracellular and intracellular bacterial burdens.

Sit@F(AM) treatment group showed significant advantages in eliminating *in vivo* persisters (Figure 5b-d). In the free Sit group, a substantial number of extracellular bacteria remained, with an average residual count of approximately 10^3 CFU. In contrast, Sit@F(AM) treatment markedly reduced bacterial burden, with almost no detectable extracellular bacteria. Notably, no intracellular persisters were recovered from any mice treated with Sit@F(AM), whereas intracellular bacterial loads in the free Sit group reached approximately 10^3 CFU. This pronounced difference is likely attributable to the targeted delivery capabilities of the F(AM) *in vivo*. First, F(AM) exhibits strong targeting and cellular uptake properties, enabling drug accumulation both at infection sites and within host cells, thereby overcoming the membrane transport and cellular barrier limitations faced by conventional antibiotics. Second, Sit@F(AM) enables on-site release in infected microenvironments, providing sustained Sit release and maintaining a high local drug concentration, which enhances the clearance of persisters.

https://doi.org/10.1021/acsami.5c11777
ACS Appl. Mater. Interfaces XXXX, XXX, XXX−XXX

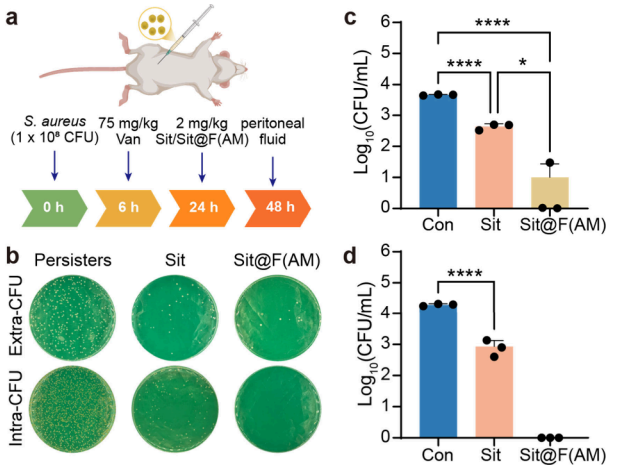

Figure 5. *In vivo* antibacterial evaluation of Sit@F(AM). (a) Mouse peritoneal model of bacterial persistence. Mice were intraperitoneally injected with *S. aureus*, and after 6 h, administered Van (75 mg/kg) to induce bacterial persistence. Subsequently, mice received 2 mg/kg of either free Sit or Sit@F(AM) and were treated for 24 h. Peritoneal lavage was then collected to quantify extracellular and intracellular bacterial loads. (b) Representative CFU images of extracellular and intracellular bacterial burden. (c) Quantification of extracellular bacterial burden in the peritonitis model. (d) Quantification of intracellular bacterial burden; no detectable persisters were observed in the Sit@F(AM)-treated group. $n = 3$, data are expressed as the mean ± SD *t* test, $^{****}p < 0.0001$, $^{*}p < 0.05$.

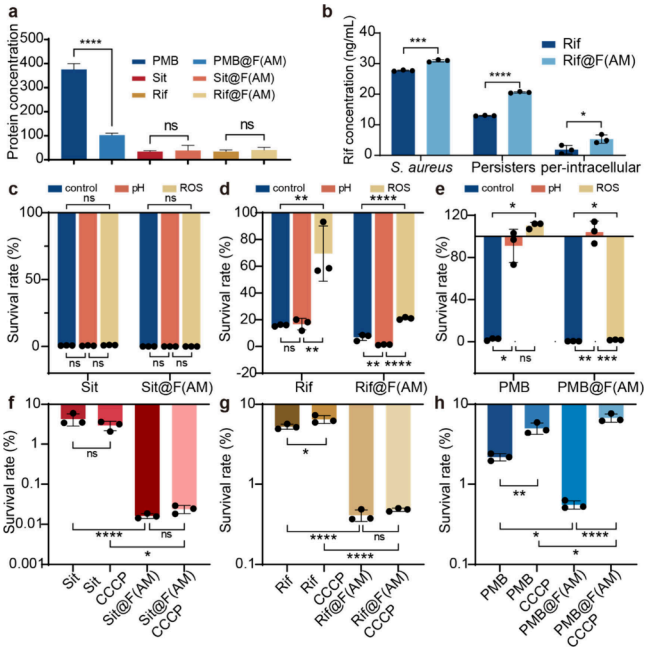

Figure 6. Mechanistic insights into bacterial elimination mediated by F(AM) NPs. (a) Protein leakage assay of persisters after treatment with free drugs or the NPs. (b) ELISA-based measurement of local Rif and Rif@F(AM) concentrations in regular planktonic bacteria, planktonic persisters, and intracellular persisters. (c) Comparison of the clearance efficacy of Sit and Sit@F(AM) against persisters under acidic and oxidative stress conditions. (d) Comparison of the clearance efficacy of Rif and Rif@F(AM) under intracellular acidic and oxidative stress conditions. (e) Comparison of the clearance efficacy of PMB and PMB@F(AM) under intracellular acidic and oxidative stress conditions. (f–h) Survival rates of persisters under metabolic suppression following treatment with free or nano-encapsulated antibiotics. $n = 3$, data are expressed as the mean ± SD. Tukey's test, $^{****}p < 0.0001$, $^{***}p < 0.001$, $^{**}p < 0.01$, $^{*}p < 0.05$, $^{ns}p > 0.05$.

3.9. Mechanistic Insights into F(AM) Enhanced Antibiotic Activity against Persisters. F(AM) serves as a robust platform for delivering antibiotics, potentially improving interactions with persisters by enhancing drug accessibility, amplifying drug activity via carrier effects, and mitigating the adverse microenvironmental conditions within bacterial niches that compromise drug efficacy. To elucidate the bactericidal mechanisms of these nanodrug formulations, an intracellular delivery and stability study of drug-loaded F(AM) NPs was performed.

To evaluate whether F(AM) encapsulation alters the intrinsic antibacterial activity of the antibiotics, their mechanisms of action against persistent bacteria were assessed and validated. Protein leakage analysis in persistent bacteria (Figure 6a, S15) revealed that both Sit and Rif induced minimal protein leakage, with negligible differences observed between their free and encapsulated forms. As Sit and Rif primarily exert their effects by inhibiting nucleic acid synthesis, targeting DNA topoisomerase and RNA polymerase respectively, these results indicate that F(AM) improves the intracellular delivery efficiency of Sit and Rif without altering their inherent mechanisms of action. In contrast, PMB exerts its bactericidal effect by disrupting bacterial membranes, leading to substantial protein leakage. Interestingly, PMB@F(AM) showed a markedly reduced leakage effect. We speculate this indicates a mismatch between pharmacodynamics of PMB and the release profile of the F(AM) carrier. PMB relies on achieving a high peak concentration within a short time frame to rapidly disrupt bacterial membranes, whereas F(AM) facilitates sustained drug release. Additionally, the persister-targeting effect of F(AM) may alter or interfere with the membrane-disrupting activity of PMB against persisters.

A common limitation of antibiotics is their inability to accumulate at bacterial sites or sustain effective local concentrations, particularly within intracellular environments. To evaluate whether F(AM) enhances antibiotic enrichment and efficacy, the intracellular concentration of Rif was quantified (Figure S16). Rif@F(AM) exhibited significantly higher accumulation and local concentrations in planktonic *S. aureus* persisters (1.59-fold, **** $p < 0.0001$) compared to free Rif, consistent with trends observed in the overall planktonic population (Figure 6b). In intracellular persisters, a marked reduction in intracellular concentration was observed for free Rif, likely due to its poor intracellular retention and limited accumulation capacity in this compartment. In contrast, Rif@F(AM) achieved improved enrichment relative to free Rif, with an approximately 2.9-fold increase in intracellular concentration ($^{*}p = 0.0381$), demonstrating the advantage of its targeted delivery capability. These results indicated that F(AM) reshaped the pharmacokinetic profile of Rif, enabling targeted delivery and localized release, thereby enhancing drug-target interactions and bactericidal efficacy.

Beyond intracellular drug concentrations, microenvironmental factors such as acidity and oxidative stress critically modulate antibiotic efficacy and bacterial persistence. To investigate this, bactericidal activities of drug-loaded F(AM) formulations were assessed under lysosome-mimicking acidic

https://doi.org/10.1021/acsami.5c11777
ACS Appl. Mater. Interfaces XXXX, XXX, XXX−XXX

(pH 5.5) and oxidative stress (H_2O_2) conditions.[65] Sit maintained structural stability and bactericidal potency despite stress-induced deepened dormancy in persisters, attributable to its DNA topoisomerase-targeting mechanism with minimal metabolic dependence (Figure 6c).[66] Conversely, oxidative stress enhanced antioxidant defenses and preserved transcriptional activity in persisters, indirectly reducing the efficacy of Rif, which inhibits RNA polymerase-mediated transcription.[67] Rif activity decreased markedly the survival rate from 15.8% to 69.5% (** p = 0.0040, Figure 6d), whereas F(AM)-mediated delivery restored bactericidal efficacy, the survival rate from 6.9% to 21.0% (**** $p < 0.0001$), highlighting the capacity of targeted delivery to overcome oxidative stress-adaptive defenses. Notably, PMB lost bactericidal activity under both stress conditions (Figure 6e). Acidic pH diminished membrane surface charge, weakening electrostatic interactions essential for PMB binding, while oxidative stress-induced depolarization disrupted membrane potential-dependent killing mechanisms. F(AM) delivery restored PMB activity under oxidative but not acidic conditions, paralleling the trend observed with Rif. This finding also clarifies why F(AM) NPs enhanced intracellular accumulation of PMB (Figure S14) without a corresponding significant improvement in bactericidal activity. Acidic lysosomes accelerated the release of PMB from F(AM) NPs, while the acidic environment concurrently inactivated PMB.

To further evaluate the impact of reduced bacterial metabolic activity on antibiotic efficacy, persistent *S. aureus* were treated with carbonyl cyanide CCCP to deplete adenosine triphosphate (ATP) levels and dissipate the proton motive force. Under these conditions, Sit maintained stable bactericidal activity, and Sit@F(AM) also showed no significant change (Figure 6f). These results suggest that Sit exerts its bactericidal effects independently of bacterial energy metabolism. In contrast, the bactericidal activity of free Rif was moderately reduced after CCCP treatment (survival rata from 5.26% to 6.50%), showing a statistically significant but limited decline (*p = 0.0279), while Rif@F(AM) largely preserved its antibacterial potency (Figure 6g). Rif shows a partial dependence on metabolic activity for optimal efficacy, which can be mitigated through targeted delivery via F(AM). As expected, PMB was highly sensitive to metabolic disruption, with both free PMB and PMB@F(AM) exhibiting markedly reduced bactericidal activity following CCCP treatment (Figure 6h). This can be attributed to the mechanism of PMB, which depends on electrostatic interactions with membrane lipopolysaccharides and subsequent membrane depolarization. A diminished proton motive force likely interferes with membrane binding and disrupts its membrane-targeting activity, leading to significant loss of bactericidal function.

Accordingly, the host cell membrane represents a critical barrier to antibiotic penetration, restricting intracellular accumulation and diminishing efficacy against intracellular persisters. F(AM) facilitates targeted intracellular delivery and enhances antibiotic retention, thereby improving the elimination of intracellular persisters. Besides, the physicochemical properties of antibiotics significantly affect their membrane permeability, intracellular distribution, and stability under hostile microenvironmental conditions such as acidity and oxidative stress. Furthermore, considering the transcriptionally active yet translationally repressed state of persisters, nucleic acid synthesis inhibitors may provide distinct therapeutic advantages for eradicating these tolerant subpopulations within host cell.

4. CONCLUSIONS

Summary, we proposed an on-site delivery strategy to enhance the intracellular antibacterial efficacy against *S. aureus* persisters using a versatile F(AM) platform. The F(AM) platform exhibited dual-targeting capability toward host cells and intracellular persisters, efficiently penetrating cellular barriers and achieving on-site antibiotic delivery at the intracellular bacterial niches. This strategy markedly increased intracellular drug accumulation, protected antibiotics from hostile microenvironments, and overcame microenvironment-induced bacterial metabolic adaptation. As a result, antibiotic-loaded F(AM) NPs achieved superior eradication of intracellular persisters both *in vitro* and *in vivo*, significantly outperforming free antibiotics. This study not only establishes a robust on-site delivery strategy for eliminating intracellular persisters but also offers mechanistic insights into optimizing intracellular antibiotic therapy.

■ ASSOCIATED CONTENT

Supporting Information

The Supporting Information is available free of charge at https://pubs.acs.org/doi/10.1021/acsami.5c11777.

Validation of persister model construction using GFP-*E. coli* (Figure S1); Van induction followed by Van fails to reduce persistent bacteria (Figure S2); Synthetic routes of the F, A_{Boc}, M_{OAc}, PF, and F(AM) (Scheme S1); ^{1}H NMR spectra of (a) F, (b) A_{Boc}, and (c) M_{OAc} (400 MHz, DMSO-d_6) (Figure S3); ^{1}H NMR spectrum of the PF (400 MHz, DMSO-d_6) (Figure S4); ^{1}H NMR spectrum of F($A_{Boc}M_{OAc}$) (400 MHz, DMSO-d_6) (Figure S5); ^{1}H NMR spectrum of F(AM) (400 MHz, DMSO-d_6) (Figure S6); 1H NMR spectrum of FA (400 MHz, DMSO-d_6) (Figure S7); GPC analysis of PF and F(AM) (Table S1); Zete of F(AM) NPs, PMB@F(AM) NPs, Sit@F(AM) NPs and Rif@F(AM) NPs (Figure S8); The cell cytotoxicity of PMB, Sit, Rif, PMB@F(AM) NPs, Sit@F(AM) NPs and Rif@F(AM) NPs (Figure S9); Standard curve of (a) PMB, (b) Sit and (c) Rif (Figure S10); DLC and DLE of the (a) PMB@F(AM) NPs, (b) Sit@F(AM) NPs and (c) Rif@F(AM) NPs (Table S2); Cell phagocytosis (Figure S11); Standard curve of NR@F(AM) NPs (Figure S12); MBC of (a) PMB and PMB@F(AM) NPs, (b) Sit and Sit@F(AM) NPs and (c) Rif and Rif@F(AM) NPs (Figure S13); Differences in cell uptake between PMB and PMB@F(AM) at different time (Figure S14); BCA protein leakage standard curve (Figure S15); Standard curve for local concentration of Rif (enzyme immunoassay) (Figure S16). (PDF)

■ AUTHOR INFORMATION

Corresponding Authors

Guofeng Li − *State Key Laboratory of Organic−Inorganic Composites, Beijing University of Chemical Technology, Beijing 100029, P. R. China;* orcid.org/0000-0002-4101-0059; Email: ligf@mail.buct.edu.cn

Xing Wang − *State Key Laboratory of Organic−Inorganic Composites, Beijing University of Chemical Technology,*

https://doi.org/10.1021/acsami.5c11777
ACS Appl. Mater. Interfaces XXXX, XXX, XXX−XXX

Beijing 100029, P. R. China; orcid.org/0000-0002-9990-1479; Email: wangxing@mail.buct.edu.cn

Authors

Zibo Yin − *State Key Laboratory of Organic−Inorganic Composites, Beijing University of Chemical Technology, Beijing 100029, P. R. China*

Diandian Huang − *State Key Laboratory of Organic−Inorganic Composites, Beijing University of Chemical Technology, Beijing 100029, P. R. China*

Dongdong Zhao − *State Key Laboratory of Organic−Inorganic Composites, Beijing University of Chemical Technology, Beijing 100029, P. R. China*

Yizhen You − *State Key Laboratory of Organic−Inorganic Composites, Beijing University of Chemical Technology, Beijing 100029, P. R. China*

Jiaqi Gu − *State Key Laboratory of Organic−Inorganic Composites, Beijing University of Chemical Technology, Beijing 100029, P. R. China*

Wensheng Xie − *State Key Laboratory of Organic−Inorganic Composites, Beijing University of Chemical Technology, Beijing 100029, P. R. China*

T. Fintan Moriarty − *AO Research Institute Davos, 7270 Davos, Switzerland;* orcid.org/0000-0003-2307-0397

Complete contact information is available at: https://pubs.acs.org/10.1021/acsami.5c11777

Author Contributions

Z. Yin: Data curation, Formal analysis, Conceptualization, Visualization, Writing-Original draft preparation. D. Huang: Methodology. D. Zhao: Methodology, Conceptualization. Y. You: Data Curation. J. Gu: Validation. W. Xie: Data Curation. T. Fintan Moriarty: Data Curation. G. Li: Conceptualization, Supervision, Visualization, Writing-Original draft preparation, Writing-Review and Editing, Funding acquisition. X. Wang: Conceptualization, Supervision, Writing-Review and Editing, Funding acquisition.

Notes

The authors declare no competing financial interest.

■ ACKNOWLEDGMENTS

This research was supported by the National Natural Science Foundation of China (22275013, 52273118), the Fundamental Research Funds for the Central Universities (PY2508, QNTD2023-01), the Innovation& Transfer Fund of Peking University Third Hospital (BYSYZHKC107).

■ REFERENCES

(1) Fang, F. C.; Frawley, E. R.; Tapscott, T.; Vázquez-Torres, A. Bacterial Stress Responses during Host Infection. *Cell Host Microbe* **2016**, *20* (2), 133−143.

(2) Masters, E. A.; Ricciardi, B. F.; Bentley, K. L. D. M.; Moriarty, T. F.; Schwarz, E. M.; Muthukrishnan, G. Skeletal Infections: Microbial Pathogenesis, Immunity and Clinical Management. *Nat. Rev. Microbiol.* **2022**, *20* (7), 385−400.

(3) Kamaruzzaman, N. F.; Kendall, S.; Good, L. Targeting the Hard to Reach: Challenges and Novel Strategies in the Treatment of Intracellular Bacterial Infections. *Br. J. Pharmacol.* **2017**, *174* (14), 2225−2236.

(4) Howden, B. P.; Giulieri, S. G.; Wong Fok Lung, T.; Baines, S. L.; Sharkey, L. K.; Lee, J. Y. H.; Hachani, A.; Monk, I. R.; Stinear, T. P. Staphylococcus Aureus Host Interactions and Adaptation. *Nat. Rev. Microbiol.* **2023**, *21* (6), 380−395.

(5) Choi, V.; Rohn, J. L.; Stoodley, P.; Carugo, D.; Stride, E. Drug Delivery Strategies for Antibiofilm Therapy. *Nat. Rev. Microbiol.* **2023**, *21* (9), 555−572.

(6) Tian, J.-H.; Huang, S.; Wang, Z.-H.; Li, J.-J.; Song, X.; Jiang, Z.-T.; Shi, B.-S.; Zhao, Y.-Y.; Zhang, H.-Y.; Wang, K.-R.; Hu, X.-Y.; Zhang, X.; Guo, D.-S. Supramolecular Discrimination and Diagnosis-Guided Treatment of Intracellular Bacteria. *Nat. Commun.* **2025**, *16* (1), 1016.

(7) Huang, Z.; Zhang, D.; Gu, Q.; Miao, J.; Cen, X.; Golodok, R. P.; Savich, V. V.; Ilyushchenko, A. P.; Zhou, Z.; Wang, R. One-Step Coordination of Metal-Phenolic Networks as Antibacterial Coatings with Sustainable and Controllable Copper Release for Urinary Catheter Applications. *RSC Adv.* **2022**, *12* (25), 15685−15693.

(8) Yu, C.; Lu, Q.; Wang, Y.; Liu, Z.; Gnanasekar, S.; D'Amora, U.; Kang, E.-T.; Xu, L.; Xu, J.; Rao, X. Spindle-Shaped Multifunctional Nanozymes with NIR-Enhanced Catalytic Activity for Treating Methicillin-Resistant *Staphylococcus Aureus* (MRSA)-Infected Wounds through Bacterial Cuproptosis-like Death. *ACS Appl. Mater. Interfaces* **2025**, *17*, 31993.

(9) Li, G.; Feng, Z.; Hou, Z.; Chen, R.; Cui, H.; Wang, T.; Li, P. Dual-Cascade Responsive H_2 Se Delivery Nanogels Bearing Selenobenzamide as H_2 Se Donor for the Treatment of Multidrug Resistant Bacteria Infections. *Adv. Funct. Mater.* **2025**, *35* (19), 2418229.

(10) Garzoni, C.; Kelley, W. L. Staphylococcus Aureus: New Evidence for Intracellular Persistence. *Trends Microbiol.* **2009**, *17* (2), 59−65.

(11) Fisher, R. A.; Gollan, B.; Helaine, S. Persistent bacterial infections and persister cells. *Nat. Rev. Microbiol.* **2017**, *15* (8), 453−464.

(12) Dadole, I.; Blaha, D.; Personnic, N. The macrophage-bacterium mismatch in persister formation. *Trends Microbiol.* **2024**, *32* (10), 944−956.

(13) Yang, S.; Han, X.; Yang, Y.; Qiao, H.; Yu, Z.; Liu, Y.; Wang, J.; Tang, T. Bacteria-Targeting Nanoparticles with Microenvironment-Responsive Antibiotic Release To Eliminate Intracellular *Staphylococcus Aureus* and Associated Infection. *ACS Appl. Mater. Interfaces* **2018**, *10* (17), 14299−14311.

(14) Maghrebi, S.; Thomas, N.; Prestidge, C. A.; Joyce, P. Inulin-Lipid Hybrid (ILH) Microparticles Promote pH-Triggered Release of Rifampicin within Infected Macrophages. *Drug Delivery Transl. Res.* **2023**, *13* (6), 1716−1729.

(15) Wu, Y.; Vulić, M.; Keren, I.; Lewis, K. Role of Oxidative Stress in Persister Tolerance. *Antimicrob. Agents Chemother.* **2012**, *56* (9), 4922−4926.

(16) Conlon, B. P.; Rowe, S. E.; Gandt, A. B.; Nuxoll, A. S.; Donegan, N. P.; Zalis, E. A.; Clair, G.; Adkins, J. N.; Cheung, A. L.; Lewis, K. Persister Formation in Staphylococcus Aureus Is Associated with ATP Depletion. *Nat. Microbiol.* **2016**, *1* (5), 16051.

(17) Rowe, S. E.; Wagner, N. J.; Li, L.; Beam, J. E.; Wilkinson, A. D.; Radlinski, L. C.; Zhang, Q.; Miao, E. A.; Conlon, B. P. Reactive Oxygen Species Induce Antibiotic Tolerance during Systemic Staphylococcus Aureus Infection. *Nat. Microbiol.* **2020**, *5* (2), 282−290.

(18) Peyrusson, F.; Tulkens, P. M.; Van Bambeke, F. Cellular Pharmacokinetics and Intracellular Activity of Gepotidacin against Staphylococcus Aureus Isolates with Different Resistance Phenotypes in Models of Cultured Phagocytic Cells. *Antimicrob. Agents Chemother.* **2018**, *62* (4), No. e02245-17.

(19) Wang, C.; Jin, L. Microbial persisters and host: recent advances and future perspectives. *Crit. Rev. Microbiol.* **2023**, *49* (5), 658−670.

(20) Maisonneuve, E.; Gerdes, K. Molecular Mechanisms Underlying Bacterial Persisters. *Cell* **2014**, *157* (3), 539−548.

(21) Lewis, K. Persister Cells, Dormancy and Infectious Disease. *Nat. Rev. Microbiol.* **2007**, *5* (1), 48−56.

(22) Wainwright, J.; Hobbs, G.; Nakouti, I. Persister Cells: Formation, Resuscitation and Combative Therapies. *Arch. Microbiol.* **2021**, *203* (10), 5899−5906.

(23) Bakkeren, E.; Diard, M.; Hardt, W.-D. Evolutionary Causes and Consequences of Bacterial Antibiotic Persistence. *Nat. Rev. Microbiol.* **2020**, *18* (9), 479−490.
(24) Bollen, C.; Louwagie, E.; Verstraeten, N.; Michiels, J.; Ruelens, P. Environmental, Mechanistic and Evolutionary Landscape of Antibiotic Persistence. *EMBO Rep.* **2023**, *24* (8), No. e57309.
(25) Peyrusson, F.; Varet, H.; Nguyen, T. K.; Legendre, R.; Sismeiro, O.; Coppée, J.-Y.; Wolz, C.; Tenson, T.; Van Bambeke, F. Intracellular Staphylococcus Aureus Persisters upon Antibiotic Exposure. *Nat. Commun.* **2020**, *11* (1), 2200.
(26) Yin, Z.; Huang, D.; Kuhn, E. M. A.; Moriarty, T. F.; Li, G.; Wang, X. Unraveling Persistent Bacteria: Formation, Niches, and Eradication Strategies. *Microbiol. Res.* **2025**, *297*, 128189.
(27) Jia, J.; Zheng, M.; Zhang, C.; Li, B.; Lu, C.; Bai, Y.; Tong, Q.; Hang, X.; Ge, Y.; Zeng, L.; Zhao, M.; Song, F.; Zhang, H.; Zhang, L.; Hong, K.; Bi, H. Killing of *Staphylococcus Aureus* Persisters by a Multitarget Natural Product Chrysomycin A. *Sci. Adv.* **2023**, *9* (31), No. eadg5995.
(28) Conlon, B. P.; Nakayasu, E. S.; Fleck, L. E.; LaFleur, M. D.; Isabella, V. M.; Coleman, K.; Leonard, S. N.; Smith, R. D.; Adkins, J. N.; Lewis, K. Activated ClpP Kills Persisters and Eradicates a Chronic Biofilm Infection. *Nature* **2013**, *503* (7476), 365−370.
(29) Zhou, C.; Zhou, Y.; Zheng, Y.; Yu, Y.; Yang, K.; Chen, Z.; Chen, X.; Wen, K.; Chen, Y.; Bai, S.; Song, J.; Wu, T.; Lei, E.; Wan, M.; Cai, Q.; Ma, L.; Wong, W.-L.; Bai, Y.; Zhang, C.; Feng, X. Amphiphilic Nano-Swords for Direct Penetration and Eradication of Pathogenic Bacterial Biofilms. *ACS Appl. Mater. Interfaces* **2023**, *15* (16), 20458−20473.
(30) Allison, K. R.; Brynildsen, M. P.; Collins, J. J. Metabolite-Enabled Eradication of Bacterial Persisters by Aminoglycosides. *Nature* **2011**, *473* (7346), 216−220.
(31) Peng, B.; Su, Y.; Li, H.; Han, Y.; Guo, C.; Tian, Y.; Peng, X. Exogenous Alanine and/or Glucose plus Kanamycin Kills Antibiotic-Resistant Bacteria. *Cell Metab.* **2015**, *21* (2), 249−262.
(32) Lebeaux, D.; Chauhan, A.; Létoffé, S.; Fischer, F.; De Reuse, H.; Beloin, C.; Ghigo, J.-M. pH-Mediated Potentiation of Aminoglycosides Kills Bacterial Persisters and Eradicates In Vivo Biofilms. *J. Infect. Dis.* **2014**, *210* (9), 1357−1366.
(33) Mohamed, M. F.; Brezden, A.; Mohammad, H.; Chmielewski, J.; Seleem, M. N. Targeting Biofilms and Persisters of ESKAPE Pathogens with P14KanS, a Kanamycin Peptide Conjugate. *Biochim. Biophys. Acta BBA - Gen. Subj.* **2017**, *1861* (4), 848−859.
(34) Chen, X.; Zhang, M.; Zhou, C.; Kallenbach, N. R.; Ren, D. Control of Bacterial Persister Cells by Trp/Arg-Containing Antimicrobial Peptides. *Appl. Environ. Microbiol.* **2011**, *77* (14), 4878−4885.
(35) Kim, W.; Steele, A. D.; Zhu, W.; Csatary, E. E.; Fricke, N.; Dekarske, M. M.; Jayamani, E.; Pan, W.; Kwon, B.; Sinitsa, I. F.; Rosen, J. L.; Conery, A. L.; Fuchs, B. B.; Vlahovska, P. M.; Ausubel, F. M.; Gao, H.; Wuest, W. M.; Mylonakis, E. Discovery and Optimization of nTZDpa as an Antibiotic Effective Against Bacterial Persisters. *ACS Infect. Dis.* **2018**, *4* (11), 1540−1545.
(36) Bhando, T.; Bhattacharyya, T.; Gaurav, A.; Akhter, J.; Saini, M.; Gupta, V. K.; Srivastava, S. K.; Sen, H.; Navani, N. K.; Gupta, V.; Biswas, D.; Chaudhry, R.; Pathania, R. Antibacterial Properties and in Vivo Efficacy of a Novel Nitrofuran, IITR06144, against MDR Pathogens. *J. Antimicrob. Chemother.* **2019**, dkz428.
(37) Zhang, K.; Du, Y.; Si, Z.; Liu, Y.; Turvey, M. E.; Raju, C.; Keogh, D.; Ruan, L.; Jothy, S. L.; Reghu, S.; Marimuthu, K.; De, P. P.; Ng, O. T.; Mediavilla, J. R.; Kreiswirth, B. N.; Chi, Y. R.; Ren, J.; Tam, K. C.; Liu, X.-W.; Duan, H.; Zhu, Y.; Mu, Y.; Hammond, P. T.; Bazan, G. C.; Pethe, K.; Chan-Park, M. B. Enantiomeric Glycosylated Cationic Block Co-Beta-Peptides Eradicate Staphylococcus Aureus Biofilms and Antibiotic-Tolerant Persisters. *Nat. Commun.* **2019**, *10* (1), 4792.
(38) Zhan, W.; Xu, L.; Liu, Z.; Liu, X.; Gao, G.; Xia, T.; Cheng, X.; Sun, X.; Wu, F.; Yu, Q.; Liang, G. Tandem Guest-Host-Receptor Recognitions Precisely Guide Ciprofloxacin to Eliminate Intracellular *Staphylococcus Aureus*. *Angew. Chem., Int. Ed.* **2023**, *62* (32), No. e202306427.
(39) Lu, K.; Qu, Y.; Lin, Y.; Li, L.; Wu, Y.; Zou, Y.; Chang, T.; Zhang, Y.; Yu, Q.; Chen, H. A Photothermal Nanoplatform with Sugar-Triggered Cleaning Ability for High-Efficiency Intracellular Delivery. *ACS Appl. Mater. Interfaces* **2022**, *14* (2), 2618−2628.
(40) Maghrebi, S.; Joyce, P.; Jambhrunkar, M.; Thomas, N.; Prestidge, C. A. Poly(Lactic-*Co*-Glycolic) Acid-Lipid Hybrid Microparticles Enhance the Intracellular Uptake and Antibacterial Activity of Rifampicin. *ACS Appl. Mater. Interfaces* **2020**, *12* (7), 8030−8039.
(41) Subramaniam, S.; Joyce, P.; Prestidge, C. A. Liquid Crystalline Lipid Nanoparticles Improve the Antibacterial Activity of Tobramycin and Vancomycin against Intracellular Pseudomonas Aeruginosa and Staphylococcus Aureus. *Int. J. Pharm.* **2023**, *639*, 122927.
(42) Delcour, A. H. Outer Membrane Permeability and Antibiotic Resistance. *Biochim. Biophys. Acta BBA - Proteins Proteomics* **2009**, *1794* (5), 808−816.
(43) Blair, J. M.; Richmond, G. E.; Piddock, L. J. Multidrug Efflux Pumps in Gram-Negative Bacteria and Their Role in Antibiotic Resistance. *Future Microbiol.* **2014**, *9* (10), 1165−1177.
(44) Rayamajhi, S.; Marchitto, J.; Nguyen, T. D. T.; et al. pH-Responsive Cationic Liposome for Endosomal Escape-Mediated Drug Delivery. *Colloids Surf. B Biointerfaces* **2020**, *188*, 110804.
(45) Juarez, P.; Broutin, I.; Bordi, C.; Plésiat, P.; Llanes, C. Constitutive Activation of MexT by Amino Acid Substitutions Results in MexEF-OprN Overproduction in Clinical Isolates of Pseudomonas Aeruginosa. *Antimicrob. Agents Chemother.* **2018**, *62* (5), No. e02445-17.
(46) Subramaniam, S.; Joyce, P.; Thomas, N.; Prestidge, C. A. Bioinspired Drug Delivery Strategies for Repurposing Conventional Antibiotics against Intracellular Infections. *Adv. Drug Delivery Rev.* **2021**, *177*, 113948.
(47) Lesbats, J.; Brillac, A.; Reisz, J. A.; Mukherjee, P.; Lhuissier, C.; Fernández-Monreal, M.; Dupuy, J.-W.; Sequeira, A.; Tioli, G.; De La Calle Arregui, C.; Pinson, B.; Wendisch, D.; Rousseau, B.; Efeyan, A.; Sander, L. E.; D'Alessandro, A.; Garaude, J. Macrophages Recycle Phagocytosed Bacteria to Fuel Immunometabolic Responses. *Nature* **2025**, *640*, 524.
(48) Feng, W.; Li, G.; Kang, X.; Wang, R.; Liu, F.; Zhao, D.; Li, H.; Bu, F.; Yu, Y.; Moriarty, T. F.; Ren, Q.; Wang, X. Cascade-Targeting Poly(amino acid) Nanoparticles Eliminate Intracellular Bacteria via On-Site Antibiotic Delivery. *Adv. Mater.* **2022**, *34* (12), 2109789.
(49) Zhao, D.; Feng, W.; Kang, X.; Li, H.; Liu, F.; Zheng, W.; Li, G.; Wang, X. Dual-targeted poly(amino acid) nanoparticles deliver drug combinations on-site: an intracellular synergistic strategy to eliminate intracellular bacteria. *J. Mater. Chem. B* **2023**, *11* (13), 2958−2971.
(50) Helaine, S.; Kugelberg, E. Bacterial Persisters: Formation, Eradication, and Experimental Systems. *Trends Microbiol.* **2014**, *22* (7), 417−424.
(51) Balaban, N. Q.; Helaine, S.; Lewis, K.; Ackermann, M.; Aldridge, B.; Andersson, D. I.; Brynildsen, M. P.; Bumann, D.; Camilli, A.; Collins, J. J.; Dehio, C.; Fortune, S.; Ghigo, J.-M.; Hardt, W.-D.; Harms, A.; Heinemann, M.; Hung, D. T.; Jenal, U.; Levin, B. R.; Michiels, J.; Storz, G.; Tan, M.-W.; Tenson, T.; Van Melderen, L.; Zinkernagel, A. Definitions and Guidelines for Research on Antibiotic Persistence. *Nat. Rev. Microbiol.* **2019**, *17* (7), 441−448.
(52) Dengler, V.; Meier, P. S.; Heusser, R.; Berger-Bächi, B.; McCallum, N. Induction Kinetics of the Staphylococcus Aureus Cell Wall Stress Stimulon in Response to Different Cell Wall Active Antibiotics. *BMC Microbiol.* **2011**, *11* (1), 16.
(53) Tajbakhsh, G.; Golemi-Kotra, D. The Dimerization Interface in VraR Is Essential for Induction of the Cell Wall Stress Response in Staphylococcus Aureus: A Potential Druggable Target. *BMC Microbiol.* **2019**, *19* (1), 153.
(54) Blattman, S. B.; Jiang, W.; McGarrigle, E. R.; Liu, M.; Oikonomou, P.; Tavazoie, S. Identification and Genetic Dissection of Convergent Persister Cell States. *Nature* **2024**, *636* (8042), 438−446.
(55) Subramaniam, S.; Joyce, P.; Ogunniyi, A. D.; Dube, A.; Sampson, S. L.; Lehr, C.-M.; Prestidge, C. A. Minimum Information

https://doi.org/10.1021/acsami.5c11777
ACS Appl. Mater. Interfaces XXXX, XXX, XXX−XXX

for Conducting and Reporting *In Vitro* Intracellular Infection Assays. *ACS Infect. Dis.* **2024**, *10* (2), 337−349.
(56) Liu, S.; Huang, Y.; Jensen, S.; Laman, P.; Kramer, G.; Zaat, S. A. J.; Brul, S. Molecular Physiological Characterization of the Dynamics of Persister Formation in *Staphylococcus Aureus*. *Antimicrob. Agents Chemother.* **2024**, *68* (1), No. e00850-23.
(57) Yang, X.; Tang, X.; Yi, S.; Guo, T.; Liao, Y.; Wang, Y.; Zhang, X. Maltodextrin-Derived Nanoparticles Resensitize Intracellular Dormant Staphylococcus Aureus to Rifampicin. *Carbohydr. Polym.* **2025**, *348*, 122843.
(58) Mateus, A.; Matsson, P.; Artursson, P. Rapid Measurement of Intracellular Unbound Drug Concentrations. *Mol. Pharmaceutics* **2013**, *10* (6), 2467−2478.
(59) Scott, D. O.; Ghosh, A.; Di, L.; Maurer, T. S. Passive Drug Permeation through Membranes and Cellular Distribution. *Pharmacol. Res.* **2017**, *117*, 94−102.
(60) Hamill, K. M.; McCoy, L. S.; Wexselblatt, E.; Esko, J. D.; Tor, Y. Polymyxins Facilitate Entry into Mammalian Cells. *Chem. Sci.* **2016**, *7* (8), 5059−5068.
(61) Feng, W.; Chittò, M.; Xie, W.; Ren, Q.; Liu, F.; Kang, X.; Zhao, D.; Li, G.; Moriarty, T. F.; Wang, X. Poly(D-Amino Acid) Nanoparticles Target *Staphylococcal* Growth and Biofilm Disassembly by Interfering with Peptidoglycan Synthesis. *ACS Nano* **2024**, *18* (11), 8017−8028.
(62) Niu, H.; Gu, J.; Zhang, Y. Bacterial Persisters: Molecular Mechanisms and Therapeutic Development. *Signal Transduct. Target. Ther.* **2024**, *9* (1), 174.
(63) Olaitan, A. O.; Morand, S.; Rolain, J.-M. Mechanisms of Polymyxin Resistance: Acquired and Intrinsic Resistance in Bacteria. *Front. Microbiol.* **2014**, *5*. DOI: 10.3389/fmicb.2014.00643.
(64) Huang, D.; Kang, X.; Yin, Z.; Zhao, D.; Ning, Y.; Liu, H.; Li, F.; Xie, W.; Li, G.; Wang, X. On-Site Serine Delivery Drives Fermentation Pathway Reprogramming to Reverse Intracellular *Staphylococcus Aureus* Persistence. *ACS Nano* **2025**, *19*, 26075.
(65) Dai, X.; Li, Y.; Zhang, Y.; Zou, Y.; Yuan, S.; Gao, F. pH/H2O2 Dual-Responsive Macrophage-Targeted Chitosaccharides Nanoparticles to Combat Intracellular Bacterial Infection. *Colloids Surf. B Biointerfaces* **2025**, *248*, 114465.
(66) Kuhn, E. M. A.; Sominsky, L. A.; Chittò, M.; Schwarz, E. M.; Moriarty, T. F. Antibacterial Mechanisms and Clinical Impact of Sitafloxacin. *Pharmaceuticals* **2024**, *17* (11), 1537.
(67) Statsenko, V. N.; Prazdnova, E. V. Influence of Rifampicin-Resistance Mutations on the Synthesis of Antioxidant, DNA-Protective, and SOS-Inhibitory Metabolites. *Appl. Biochem. Microbiol.* **2025**, *61*, 542.

https://doi.org/10.1021/acsami.5c11777
ACS Appl. Mater. Interfaces XXXX, XXX, XXX−XXX